

Structural characterisation of solution species implicated in the palladium-catalysed Heck reaction by Pd K-edge X-ray absorption spectroscopy: palladium acetate as a catalyst precursor

John Evans,^a Lynn O'Neill,^a Vijaya L. Kambhampati,^a Graham Rayner,^a Sandra Turin,^a Anthony Genge,^a Andrew J. Dent^b and Thomas Neisius^c

^a Department of Chemistry, University of Southampton, Southampton, UK SO17 1BJ

^b CLRC Daresbury Laboratory, Warrington, UK, WA4 4AD

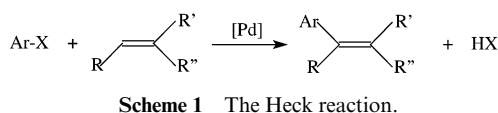
^c ESRF, PO Box 220, Grenoble cedex, F-38043, France

Received 17th January 2002, Accepted 12th March 2002

First published as an Advance Article on the web 17th April 2002

Energy dispersive EXAFS (EDE), Quick EXAFS (QEXAFS), ¹³C NMR and X-ray crystallography have been used to probe the co-ordination sphere of palladium in the course of the phosphine free Heck reaction. [Pd₂I₆][NBu₃H]₂ has been isolated from the precatalytic solution and its crystal structure determined. EDE and QEXAFS spectra of the complexes Pd(OAc)₂, Pd(PPh₃)₄ and [Pd₂I₆][NEt₃H]₂ illustrated the value of the technique in structure elucidation. EXAFS of the precatalytic solution detects [Pd₂I₆]²⁻ and no co-ordinated carbon. EXAFS of the catalytic solution shows a first co-ordination sphere of 2 carbon atoms and a second of 2–2.5 iodines. A scheme involving an equilibrium between the oxidative addition product and the olefin co-ordination species, has been proposed to explain these results.

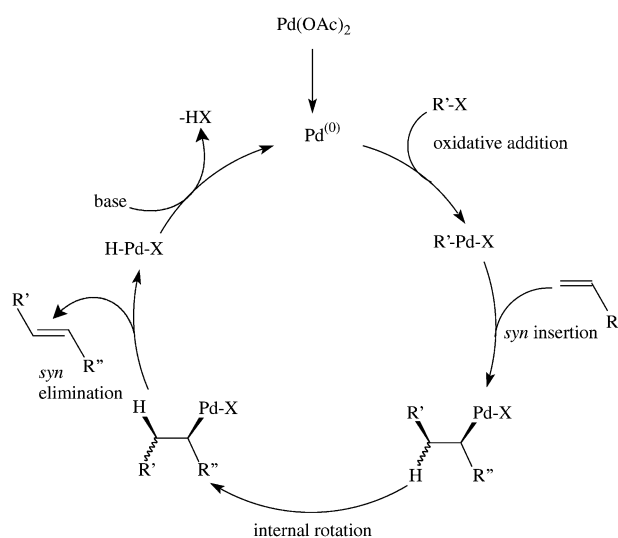
Palladium catalysed carbon–carbon bond formation is a well-established tool in synthetic organic chemistry.^{1,2} As early as 1968 R. F. Heck demonstrated that palladium acetate or mixtures of palladium acetate and triphenylphosphine could catalyse the arylation or vinylation of olefins, in what has become known as the Heck reaction, Scheme 1.³



Since the late 1980s there has been a revival of interest in the Heck reaction as a synthetic technique, its attractiveness stemming from its favourable stereo and chemoselectivity, high yields and relatively mild reaction conditions. Sequential reactions, synthesis of heterocycles and cyclic alkenes, natural product and asymmetric synthesis are just a few examples of areas where it has application.⁴

Until recently, reports concerning investigations of the mechanistic pathway were scarce and the catalysis has been assumed to proceed by an initial reduction to zero-valent palladium, followed by oxidative addition of the aryl halide.⁵ Insertion of the olefin into the metal–aryl bond follows and the product is generated by reductive elimination. The base regenerates the active palladium species, Scheme 2.

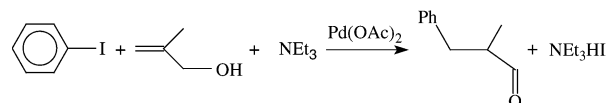
Mechanistic investigations have largely concentrated upon the role of the phosphine within the process and the initial oxidative addition step.^{6,7} To our knowledge, there has been no similar investigation of the phosphine free catalytic cycle. We have previously shown that extended X-ray absorption fine structure spectroscopy (EXAFS) and energy dispersive EXAFS (EDE) can be used to probe directly the co-ordination sphere of the metal species within homogeneous catalysis.⁸ A K-edge Pd EXAFS study of the phosphine-free Heck reaction was thus initiated, to investigate further its mechanism.



Scheme 2 Mechanism of the Heck reaction.

Results and discussion

The reaction chosen for study involved the coupling of iodo-benzene with 2-methylprop-2-en-1-ol to give 1-phenyl-2-methylpropanal, Scheme 3.¹ The reaction conditions were chosen for



Scheme 3 The Heck reaction under investigation.

the suitability of reaction conditions to study by time resolved XAFS spectroscopy. The palladium concentration was 50 mM and catalyst to reagent ratio was 1 : 20. These concentrations

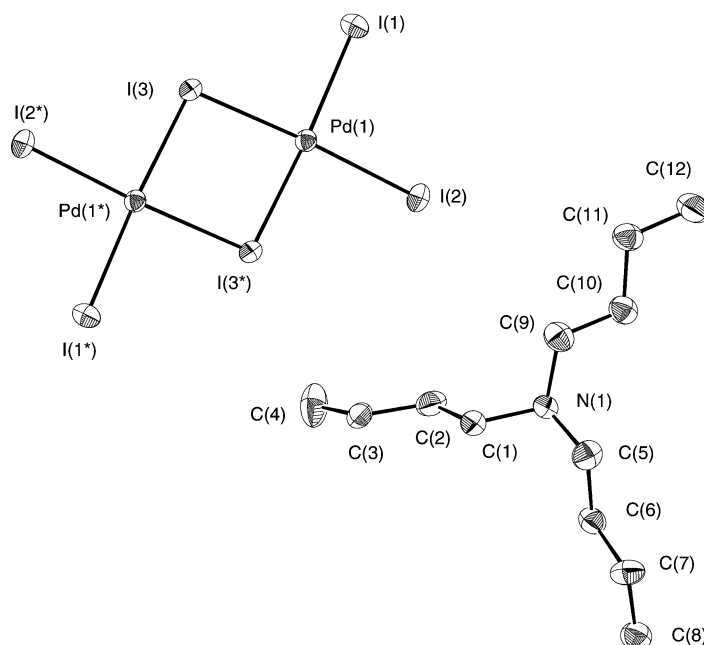


Fig. 1 View of the structure of $[\text{Pd}_2\text{I}_6][\text{NBu}_3\text{H}]_2$ with numbering scheme adopted. Ellipsoids are shown at 40% probability and atoms marked with an asterisk are related by a crystallographic inversion centre at (0.5, 1, 1).

Table 1 Crystallographic data for $[\text{Pd}_2\text{I}_6][\text{NBu}_3\text{H}]_2$

Formula	$\text{C}_{12}\text{H}_{26}\text{I}_6\text{Pd}_2\text{N}$
<i>M</i>	1346.95
Colour, morphology	Dark red, plate
Crystal dimensions/mm	$0.45 \times 0.13 \times 0.05$
Crystal system	Triclinic
Space group	$\text{P}\bar{1}$ (#2)
<i>a</i> /Å	11.779(8)
<i>b</i> /Å	11.787(8)
<i>c</i> /Å	8.690(5)
<i>a</i> /°	110.98(5)
<i>β</i> /°	100.57(6)
<i>γ</i> /°	61.67(4)
<i>U</i> /Å ³	991(1)
<i>Z</i>	1
<i>F</i> (000)	634.00
<i>D</i> /g cm ^{−3}	2.256
<i>μ</i> (Mo-Kα)/mm ^{−1}	5.593
Transmission factors (max. and min.)	0.7914–1.0000
No. of unique obs. reflections	3479
Unique obs. reflections with [<i>I</i> _o > 2.5σ(<i>I</i> _o)]	2320
No. of parameters	154
Goodness of fit	1.26
<i>R</i> (<i>F</i> _o)	0.030
<i>R</i> _w (<i>F</i> _o)	0.038
Max. residual peak/e Å ^{−3}	1.16
Max. residual trough/e Å ^{−3}	−0.69
$R = \sum (F_{\text{obs}} - F_{\text{calc}}) / \sum F_{\text{obs}} $; $R_w = \sqrt{[\sum w_i (F_{\text{obs}} - F_{\text{calc}})^2 / \sum w_i F_{\text{obs}} ^2]}$	
$\text{GOF} = [\sum (F_{\text{obs}} - F_{\text{calc}})^2 / \sigma_i] / (n - m) \approx 1$.	

initially posed a problem in terms of catalyst precipitation but this problem was overcome by choice of NMP as reaction solvent.

Addition of 2-methylprop-2-en-1-ol to a yellow solution of palladium acetate, iodobenzene, NMP (*N*-methyl-2-pyrrolidinone) and triethylamine or tributylamine produced an immediate deep red coloured solution. In the absence of the 2-methylprop-2-en-1-ol, this reaction does not proceed. The volatile reagents were removed and the remaining red solid shown to be $[\text{Pd}_2\text{I}_6][\text{NEt}_3\text{H}]_2$ or $[\text{Pd}_2\text{I}_6][\text{NBu}_3\text{H}]_2$, isolated in high yield.

Crystals of $[\text{Pd}_2\text{I}_6][\text{NBu}_3\text{H}]_2$ were grown and the crystal structure determined. The structure is shown in Fig. 1. Crystal data are given in Table 1 and selected bond lengths and angles in

Table 2 Selected bond lengths and angles for $[\text{Pd}_2\text{I}_6][\text{NBu}_3\text{H}]_2$. Atoms marked with an asterisk are at equivalent position (1 − *x*, 2 − *y*, 2 − *z*)

Pd(1)–I(1)	2.611(2)	I(1)–Pd(1)–I(2)	92.10(4)
Pd(1)–I(2)	2.5931(8)	I(1)–Pd(1)–I(3)	91.50(4)
Pd(1)–I(3)*	2.604(2)	I(1)–Pd(1)–I(3)*	176.57(3)
Pd(1)–I(3)	2.6092(8)	I(2)–Pd(1)–I(3)	176.23(3)
		I(2)–Pd(1)–I(3)*	91.30(4)
		Pd(1)–I(3)–Pd(1)*	94.89(4)
		I(3)–Pd(1)–I(3)*	85.11(4)

Table 2. The structure consists of an association of two tributyl ammonium units with a centrosymmetric di-anionic Pd_2I_6 unit. The palladium atoms are bridged by two iodine atoms.

Bond lengths and angles are within expected values when compared to related complexes.⁹ The Pd–I bond distance for terminal iodides (2.611(2) and 2.593(8) Å) and bridging iodides (2.609(8) Å) are similar indicating no lengthening of this bond through bridging. As expected the I(3)–Pd–I(3)* angle (85.11(4)°) is smaller than the I(1)–Pd–I(2) angle (92.10(4)°), a result of the constraint imposed by the bridging group. Structures of this anionic complex with other cations have been reported,¹⁰ with the nearest analogue being for the NBu_4^+ counter ion; little substantial change in the structure of $[\text{Pd}_2\text{I}_6]^{2-}$ is evident.

The above solution, with triethylamine, was heated to 75 °C, resulting in a colour change from deep red to brown–yellow. The catalysis proceeded over one hour at this temperature. All attempts to isolate the active catalytic species resulted in a conversion of the palladium complex to $[\text{Pd}_2\text{I}_6][\text{NEt}_3\text{H}]_2$. $[\text{Pd}_2\text{I}_6]^{2-}$ is a well known counter-ion^{10–12} and is clearly the most thermodynamically favourable product under these reaction conditions. Upon completion of the catalysis the solution reverts to a deep red colour from which $[\text{Pd}_2\text{I}_6][\text{NEt}_3\text{H}]_2$ was isolated as the only palladium-containing species.

Energy dispersive EXAFS (EDE) and QEXAFS studies of standard complexes

In order to illustrate the value of EXAFS and EDE towards elucidating the structure of catalytic intermediates, in solution in donor solvents, the Pd K-edge QEXAFS and EDE spectra of the standard complexes, $\text{Pd}(\text{OAc})_2$, $\text{Pd}(\text{PPh}_3)_4$ and $[\text{Pd}_2\text{I}_6][\text{NEt}_3\text{H}]_2$ were obtained. QEXAFS data of palladium acetate

Table 3 Palladium K-edge structural parameters for standard solutions: (a) palladium acetate, NMP, 70mM, QEXAFS, 6×5 minutes (averaged); (b) $\text{Pd}(\text{PPh}_3)_4$, THF, 60 mM, EDE (100×2.2 ms); (c) $[\text{Pd}_2\text{I}_6][\text{NEt}_3\text{H}]_2$, CH_3CN , 70 mM, EDE (100×6.6 ms)

Sample	Shell	CN ^a	$r/\text{\AA}$	$2\sigma^2/\text{\AA}$	A_r^c	E_r^d (eV)	$R(\%)$
(a)	O	4.37(7)	1.998(2)	0.0038(3)	0.8	-1.1(1)	24.6
(b)	P	2.79(20)	2.282(8)	0.006(1)	1.0	-2.4(2.0)	35.4
(c)	I	3.99(8)	2.678(3)	0.006(1)	1.0	-7.9(7)	13.5

^a Co-ordination number. ^b Debye–Waller factor; σ = root mean-square separation. ^c Fraction of absorption causing EXAFS ^d E_r variation in Fermi level from theory.

in NMP (70 mM) were acquired in a scan time of 30 minutes (6×5 minutes) and the average obtained. Table 3 gives the structural parameters.

The data are consistent with a first co-ordination sphere of four oxygen atoms at 1.998 Å. This is in good agreement with the crystal structure of palladium acetate where each palladium is surrounded by four bridging acetate ligands with Pd–O distances in the range of 1.973–2.014 Å.¹³ However in the crystal structure palladium acetate exists as a trimer with Pd–Pd non-bonded distances in the region of 3.105–3.203 Å. A second shell of two palladium atoms at 3.15 Å was not observed suggesting that the trimer may be broken down in NMP to a monomer. In the case of the linear trimer $[\text{Ni}(\text{acac})_2]_3$ in toluene solution, a shell could be attributed to an Ni...Ni distance,¹⁴ so it is plausible that a shell should be observable for the Pd...Pd atomic pairing in a cyclic trimer.

The EDE spectra of $\text{Pd}(\text{PPh}_3)_4$ in THF solution, 60 mM, were obtained using 100 scans of 2.2 ms integration time. Fig. 2

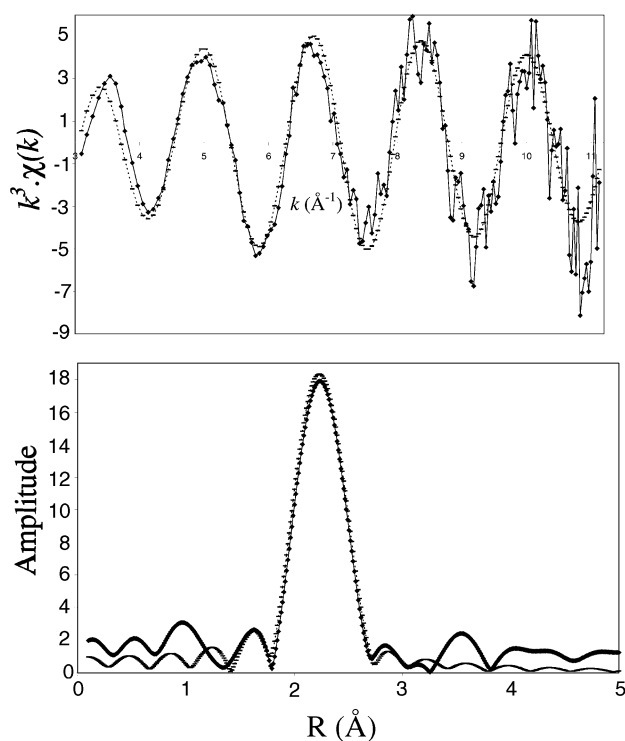


Fig. 2 The palladium K-edge k^3 -weighted EDE data and Fourier transform, (—, experimental; ----, spherical wave theory), of $\text{Pd}(\text{PPh}_3)_4$ in THF, 60mM. 100 scans, integration time: 2.2 ms.

shows EDE data and Fourier transform for the solution and Table 3 gives structural parameters. Results indicate a first co-ordination shell of three phosphorus atoms at 2.28 Å. This is in excellent agreement with experimental studies of this solution where it has been well established that $\text{Pd}(\text{PPh}_3)_4$ exists in solution primarily as $\text{Pd}(\text{PPh}_3)_3$ with a small amount of $\text{Pd}(\text{PPh}_3)_2$ present.¹⁵

EDE spectra of $[\text{Pd}_2\text{I}_6][\text{NEt}_3\text{H}]_2$ in acetonitrile, 70 mM, were obtained with 100 scans 6 ms integration times. Fig. 3 shows

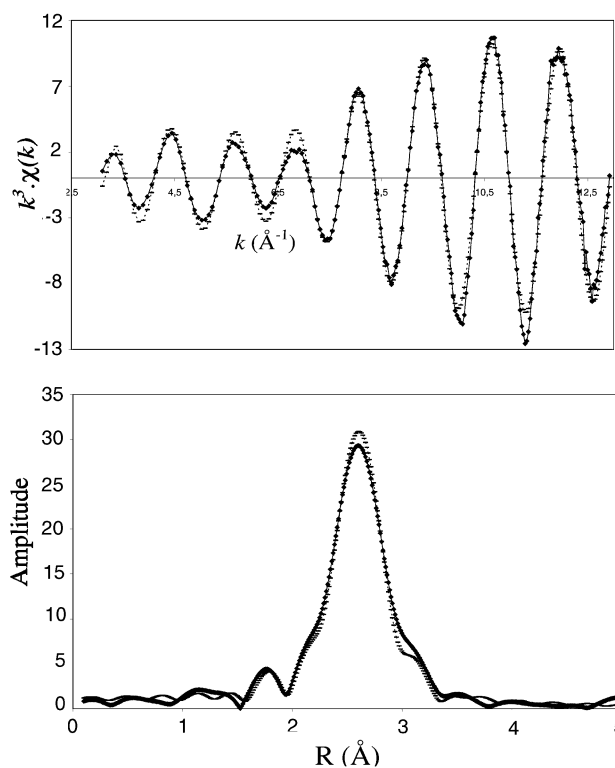


Fig. 3 The palladium K-edge k^3 -weighted EDE data and Fourier transform, (—, experimental; ----, spherical wave theory), of $[\text{Pd}_2\text{I}_6][\text{NEt}_3\text{H}]_2$ in NMP, 70 mM. 100 scans, integration time: 6 ms.

EDE data and the Fourier transform for the solution and structural parameters are given in Table 3. Results show a first co-ordination sphere of four iodines at distances of 2.676 Å from palladium. Compared with the crystal structure of $[\text{Pd}_2\text{I}_6][\text{NBu}_3\text{H}]_2$ the Pd–I distances from the EDE results are somewhat longer than those obtained from crystallography, possibly due to difficulties in calibration for this particular spectrum. There is excellent agreement between theoretical and experimental for the data and the R factor is low, 13.5%, for time-resolved data.

EDE and QEXAFS of the Heck reaction (Scheme 3)

The previous results indicate the degree of agreement that can be obtained when investigating the structures of complexes in solution using QEXAFS and EDE. The same techniques can be applied to elucidating the structures under catalytic conditions. The steps from the addition of the precursor, through the onset of catalysis to its conclusion may be monitored by increasing the temperature of the charged solution and then holding the temperature through to the completion of the catalysed reaction. It must, however, be noted that EXAFS data may be a result of the average of a number of species in solution. Data may be of poorer quality due to lower metal concentrations or possible inhomogeneity in the mixture. Despite this, valuable information can be obtained by the application of this technique to *in situ* catalytic reactions.⁸ Of particular value is the energy dispersive EXAFS (EDE) technique, where the spectra

Table 4 Palladium K-edge structural parameters for precatalytic solution at room temperature; (a) QEXAFS (4×10 minutes, averaged); (b) EDE (100 scans, integration time 6.5 ms)

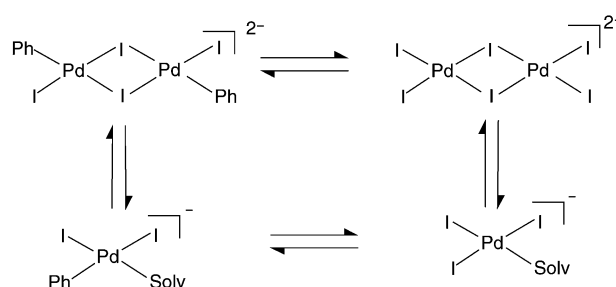
Method	Shell	CN ^a	$r/\text{\AA}$	$2\sigma^2/\text{\AA}^2$	A_f^c	E_f^d/eV	$R(\%)$
(a)	I	3.2(2)	2.62(1)	0.017(0)	1.0	-5.1(10)	39.3
(b)	I	3.2(16)	2.63(1)	0.0105(5)	1.0	-5.9(12)	27.7

^a Co-ordination number. ^b Debye–Waller factor; σ = root mean-square separation. ^c Fraction of absorption causing EXAFS. ^d E_f variation in Fermi level from theory.

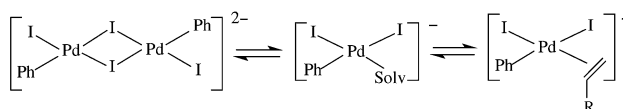
in this report were all obtained with an elapsed time of under 1 minute. This allows a snapshot of the solution to be taken at any point of the catalysis. Quick EXAFS (QEXAFS) required a five minute scan for useful data. Typically six scans of 5 minute duration were averaged. For such spectra to be valid, there should be no change in the predominant palladium species over this period. Both EDE and QEXAFS experiments were utilised to study the coupling reaction described in Scheme 3.

As noted above, when all the reagents $\{\text{Pd}(\text{OAc})_2/\text{PhI}/2\text{-methylprop-2-en-1-ol}/\text{NEt}_3\}$ in NMP are charged together a deep red colour is produced from which $[\text{Pd}_2\text{I}_6][\text{NEt}_3\text{H}]_2$ was isolated. Investigations of the precatalytic solution were required to see if this complex could be observed *in situ*. Its production may have simply been a result of the removal of volatiles. At this stage oxidative addition of iodobenzene to zerovalent palladium may have been expected to take place. At the end of the catalysis, when all the NEt_3 has reacted, the NMR resonances of $[\text{Pd}_2\text{I}_6][\text{NEt}_3\text{H}]_2$ are clearly observed. NMR data have not provided conclusive evidence of the structure of the palladium species in the precatalytic solution. QEXAFS spectra of the solution were acquired over a scan time of 40 minutes (4×10 minutes) and the average obtained. Typically EDE spectra were obtained by 100 scans and an integration time of 6.5 ms. Fig. 4 shows EDE data and Fourier

iodines at 2.62 \AA . In both experiments a shoulder on this shell is observed at 2 \AA . Attempts to fit this shell to carbon, oxygen and even phosphorus resulted in a deterioration of the fit; the Debye–Waller factor for the carbon shell was in the region of 0.058 \AA^2 . So although this shell may be indicating the presence of a lighter element, there is no definitive information about its nature. It can be concluded that in this red solution oxidative addition of the iodobenzene has probably occurred and the palladium species at this point may be an average of bridged and solvated structures, Scheme 4.

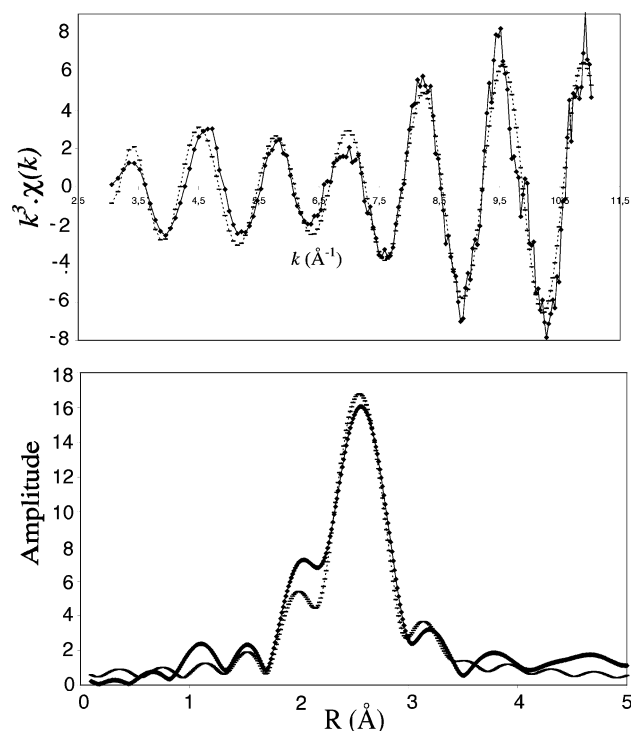
**Scheme 4** Proposed intermediates for precatalytic solution.

When the red precatalytic solution is heated to 75 $^{\circ}\text{C}$ there is a colour change to brown–yellow and catalysis proceeds over an hour. *In situ* ^{13}C NMR of this did not allow observation of the co-ordinated carbon. EDE and QEXAFS experiments were utilised for evidence of the palladium species present. QEXAFS spectra were obtained over 50 minutes (10×5 minutes) and the average obtained. EDE spectra were obtained by 100 scans and 11 ms integration time. Fig. 5 shows QEXAFS data and Fourier transform for the solution and Table 5 gives structural parameters for spectra obtained by EDE and QEXAFS. Both experiments agree well and show a first co-ordination sphere of approximately two carbons and second co-ordination sphere of ~ 2 iodines. Possible structures to explain the EXAFS data are given in Scheme 5. This shows an equilibrium between a

**Scheme 5** Proposed catalytic intermediates for catalytic solution.

dimeric oxidative addition product and the olefin co-ordination complex.

There is no direct evidence to suggest that the oxidative addition product is dimeric. Inclusion of a palladium shell in the EDE or QEXAFS, which would indicate the presence of a $\text{Pd} \cdots \text{Pd}$ shell, neither improves nor worsens the fit. However, palladium complexes do have a tendency to bridge. It is expected that the low frequency bending vibrations of the $\text{Pd}_2(\mu\text{-I})_2$ unit will provide a high dynamic Debye–Waller factor rendering the $\text{Pd} \cdots \text{Pd}$ shell difficult to detect at elevated temperatures. The opening of this bridge leaves a free co-ordination site for co-ordination by the olefin before insertion into the Pd-C σ bond, Scheme 5.

**Fig. 4** The palladium K-edge k^3 -weighted EDE data and Fourier transform, (—, experimental; ----, spherical wave theory), of precatalytic solution at room temperature. 100 scans, integration time: 6.5 ms.

transform for the solution and Table 4 gives structural parameters for spectra obtained by EDE and QEXAFS. Both experiments agree well and show a first co-ordination sphere of 3.2

Table 5 Palladium K-edge structural parameters for catalytic solution at 75 °C; (a) QEXAFS (10 × 5 minutes, averaged); (b) EDE (100 scans, integration time 11 ms)

Method	Shell	CN ^a	<i>r</i> /Å	2σ ² / <i>b</i> Å ²	<i>A_f</i> ^c	<i>E_f</i> ^d /eV	<i>R</i> (%)
(a)	C	1.5(3)	2.06(3)	0.028(3)	1.0	−5.0(12)	36.2
	I	2.3(3)	2.63(1)	0.028(1)			
(b)	C	1.6(6)	2.13(4)	0.012(8)	1.0	−3.6(26)	53
	I	1.8(3)	2.61(1)	0.014(2)			

^a Co-ordination number. ^b Debye–Waller factor; σ = root mean-square separation. ^c Fraction of absorption causing EXAFS. ^d *E_f* variation in Fermi level from theory.

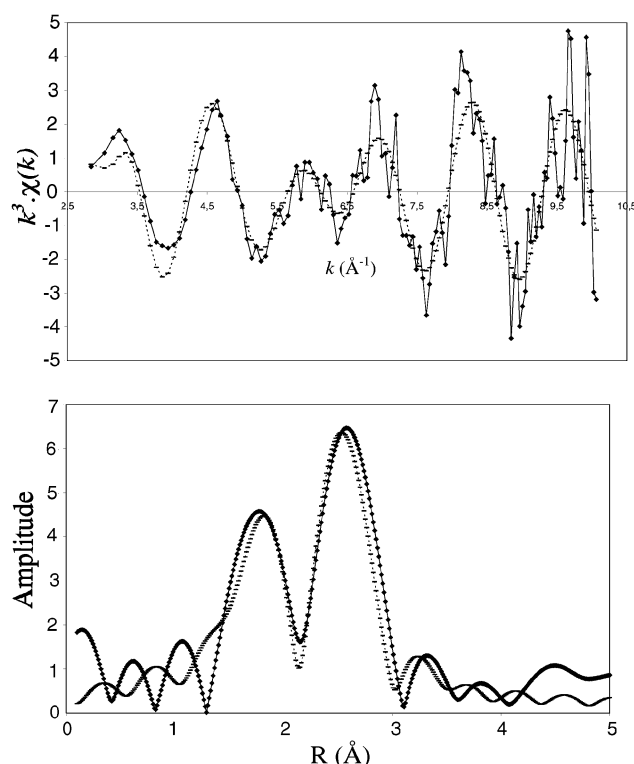


Fig. 5 The palladium K-edge k^3 -weighted QEXAFS data and Fourier transform, (—, experimental; ----, spherical wave theory), of catalytic solution at 75 °C, averaged over 50 minutes.

Conclusion

QEXAFS and EDE results of the precatalytic solution, at room temperature, support the presence of $[\text{Pd}_2\text{I}_6][\text{NEt}_3\text{H}]_2$. There is only weak evidence of the oxidative addition steps, or co-ordination by carbon, at this point. Upon heating to 75 °C the catalysis begins and the species detected by QEXAFS and EDE is a co-ordination site of 2 carbon atoms and 2 iodine atoms. This is consistent with an equilibrium of a series of structures such as the oxidative addition product and the olefin co-ordinated complex, Scheme 5. This is the step prior to the insertion of the olefin into the Pd–C σ bond in the conventional catalytic cycle.

Experimental

All manipulations were carried out under a nitrogen or argon atmosphere using standard Schlenk techniques. Anhydrous NMP, palladium acetate and 2-methylprop-2-en-1-ol were obtained from Aldrich chemicals and used directly. Iodobenzene and triethylamine were dried over calcium hydride and distilled prior to use. The progress of the catalysed reactions were monitored by extracting samples and using IR spectroscopy; these spectra were recorded on a Perkin Elmer 1600 FT-IR spectrometer, in solution using a 1.0 mm NaCl cell. The loss of iodobenzene was monitored using an absorption at 1572 cm^{-1} with the formation of 1-phenyl-2-methylprop-3-one

identified by its absorption band at 1721 cm^{-1} . Proton and ^{13}C NMR spectra were recorded on a Bruker AC 300 or AM 360 spectrometer.

EXAFS studies

QEXAFS spectra were recorded at Station 9.3 of the Synchrotron Radiation Source at the Daresbury Laboratory, UK, operating at 2 GeV (*ca.* 3.20×10^{-10} J) and an average current of 140 mA. Data were acquired in fluorescence mode using a Canberra 13-element germanium solid state detector. EDE spectra (transmission) were acquired at ID24 of the ESRF,¹⁶ Grenoble, operating at 6 GeV and an average current of 190 mA. Data were acquired in energy dispersive mode using an asymmetric cut (3°) Si(111) Laue monochromator. Energy calibration was carried out using a spectrum of a palladium foil. A masked, Peltier cooled Princeton CCD camera was used to collect the EDE data; 18 stripes of 64 pixel width, 10 of which were summed to form a single spectrum, were collected before readout. The data collection rate was limited by the readout time of the CCD chip (*ca.* 250 ms). So, 100 scans of 11 ms duration (as used for an *in situ* experiment) would involve *ca.* $11 \times 18 \times 100$ ms, of which $11 \times 10 \times 100$ ms (11 s) exposure would be processed. An additional 100×0.3 s was required for reading out the data, giving an elapsed time of *ca.* 48 s. Following this the sample was moved out of the line of the beam so that the air path was used to acquire the background (I_0) spectrum. Background subtracted EXAFS data were obtained using the program PAXAS.¹⁷ Removal of the pre-edge background was achieved using a polynomial of order 2 and the post-edge background was subtracted using a polynomial of order 6, 7 or 8. Curve fitting analyses, by least squares refinement of the non-Fourier filtered k^3 -weighted EXAFS data were carried out within EXCURV-92 and -98,¹⁸ using spherical wave methods with *ab initio* phase shifts and back scattering factors calculated in the usual manner from relativistic HF-SCF derived atomic-charge densities. The numbers of independent parameters used in the fits are within the guideline

$$N_{\text{pts}} = 2(k_{\text{max}} - k_{\text{min}})(R_{\text{max}} - R_{\text{min}})/\pi.$$

The *R* factors are defined as $(\| \chi^T - \chi^E \| k^3 dk / \| \chi^E \| k^3 dk) \times 100\%$.

Standard deviations are quoted as derived for curve fitting procedures; expectation errors on interatomic distances are between 1.0 and 1.5%.¹⁹ Errors on co-ordination numbers are *ca.* 15%.

Solutions for study were prepared in a three neck round bottomed flask and transferred by canula to a *d* = 0.5 cm (EDE) or *d* = 1 cm (fluorescence QEXAFS) stainless steel solution cell, with Kapton windows and heater cartridges attached.

$[\text{Pd}_2\text{I}_6][\text{NEt}_3\text{H}]_2$. The compound (0.38 g) was dissolved in CH_3CN (5 cm^3) and transferred directly to a 1 cm solution cell.

Precatalytic species. 2-Methylprop-2-en-1-ol (1 g) was added to palladium acetate (0.1 g), iodobenzene (2.4 g), triethylamine (1.4 g) and NMP (4 cm^3). The mixture was stirred for

10 minutes and then transferred to the solution cell. QEXAFS or EDE data were recorded over a period of 30 minutes.

Catalytic species. The above reaction mixture was heated to 50 °C and transferred to a preheated solution cell, 50 °C. The solution was heated to 75 °C and spectra recorded at this temperature over one hour. IR spectroscopy indicated that the reaction was substantially complete after that time.

In situ ^{13}C NMR studies

All spectra were recorded on a Bruker AM 360 spectrometer. The samples were run unlocked and referenced against a standard sample of NMP.

Precatalytic species. The solution used for EXAFS studies was prepared and $\text{Cr}(\text{acac})_3$ (10 mg cm^{-3}) added. The mixture was transferred to a NMR tube under an inert atmosphere. The solution was cooled to -10°C and ^{13}C spectrum accumulated over 2 hours at this temperature.

Catalytic species. The above solution was prepared and heated to 65 °C in a NMR probe. The ^{13}C spectrum was accumulated over two hours at this temperature with a printout obtained every 30 min.

Preparative studies

Isolation of $[\text{Pd}_2\text{I}_6][\text{NEt}_3\text{H}]_2$ and $[\text{Pd}_2\text{I}_6][\text{NBu}_3\text{H}]_2$. 2-Methylprop-2-en-1-ol (1 g) was added to palladium acetate (0.1 g), iodobenzene (2.4 g), and NMP (4 cm^3) and triethylamine (1.4 g) or tributylamine (2.6 g). The mixture was stirred for 30 minutes at room temperature and volatile reagents removed *in vacuo*. The resulting red solid was washed with diethyl ether to yield $[\text{Pd}_2\text{I}_6][\text{NEt}_3\text{H}]_2$ (0.17 g, 65%) or $[\text{Pd}_2\text{I}_6][\text{NBu}_3\text{H}]_2$ (0.21 g, 70%).

$[\text{Pd}_2\text{I}_6][\text{NEt}_3\text{H}]_2$. Elemental analysis: C: 11.81 (12.22); H: 2.32 (2.71); N: 23.45 (23.77)%. ^1H NMR (CDCl_3) (300 MHz): δ 1.4 (t, 3H), 3.1 (q, 2H). ^{13}C NMR (CDCl_3) (75 MHz): δ 11.63, 43.27.

$[\text{Pd}_2\text{I}_6][\text{NBu}_3\text{H}]_2$. Elemental analysis: C: 21.22 (21.40); H: 3.88 (4.16); N: 1.92 (2.08)%. ^1H NMR (CDCl_3) (300 MHz): δ 0.72 (t, 3H), 1.015–1.45(m, 6H). ^{13}C NMR (CDCl_3) (75 MHz): δ 13.94, 16.01, 28.22, 32.04.

Crystallographic studies

Dark red crystals of $[\text{Pd}_2\text{I}_6][\text{NBu}_3\text{H}]_2$ were grown from a concentrated 2-methylprop-2-en-1-ol solution. Data collection used a Rigaku AFC7S four circle diffractometer, with graphite-monochromated Mo-K α X radiation ($\lambda_{\text{max}} = 0.7103 \text{ \AA}$), $T = 150 \text{ K}$, ω – 2θ scans. The structure was solved by direct methods using PATTY,²⁰ and then developed by iterative cycles of full least squares refinement and difference Fourier syntheses which located all non-H atoms in the asymmetric unit.²¹ All non-H atoms were refined anisotropically and H atoms were placed in fixed calculated positions with $d(\text{C–H}) = 0.96 \text{ \AA}$.

CCDC reference number 168848.

See <http://www.rsc.org/suppdata/dt/b2/b200617k/> for crystallographic data in CIF or other electronic format.

Acknowledgements

We wish to thank the University of Southampton, EPSRC and BP Chemicals for financial support and the Directors and staff of the Daresbury Laboratory and ESRF for access to the facilities and for their assistance.

References

- 1 R. F. Heck, *Acc. Chem. Res.*, 1979, **12**, 146.
- 2 R. F. Heck, *Palladium Reagents in Organic Synthesis*, Academic Press, London, 1985; J. Tsuji, *Organic Synthesis with Palladium Compounds*, Springer, Berlin, 1980.
- 3 R. F. Heck, *Acc. Chem. Res.*, 1979, **12**, 146.
- 4 A. de Meijere and F. E. Meyer, *Angew. Chem., Int. Ed. Engl.*, 1994, **33**, 2379 and references therein.
- 5 W. Cabri and I. Candiani, *Acc. Chem. Res.*, 1995, **28**, 2.
- 6 C. Amatore, E. Carre, A. Jutand, M. A. M'Barki and G. Meyer, *Organometallics*, 1995, **14**, 5605; C. Amatore, E. Carre, A. Jutand and M. A. M'Barki, *Organometallics*, 1995, **14**, 1818; C. Amatore, A. Jutand and M. A. M'Barki, *Organometallics*, 1992, **11**, 3009.
- 7 T. Mandai, T. Matsumoto and J. Tsuji, *Tetrahedron Lett.*, 1993, **34**, 2513; F. Ozawa, A. Kubo and T. Hayashi, *Chem. Lett.*, 1992, 2177.
- 8 D. Bogg, M. Conyngham, J. M. Corker, A. J. Dent, J. Evans, R. C. Farrow, V. L. Kambhampati, A. F. Masters, D. N. Macleod, C. M. Ramsdale and G. Salvini, *J. Chem. Soc., Chem. Commun.*, 1996, 647; P. Andrews and J. Evans, *J. Chem. Soc., Chem. Commun.*, 1993, 1246; J. M. Corker and J. Evans, *J. Chem. Soc., Chem. Commun.*, 1991, 1104; P. Andrews, J. M. Corker, J. Evans and M. Webster, *J. Chem. Soc., Dalton Trans.*, 1994, 1337.
- 9 N. W. Alcock, W. L. Wilson and J. H. Nelson, *Inorg. Chem.*, 1993, **32**, 3193.
- 10 F. Maassarani, M. Pfeffer and G. Le Borgne, *J. Chem. Soc., Chem. Commun.*, 1987, 565; S. Chan, S.-M. Lee, Z. Lin and W.-T. Wong, *J. Organomet. Chem.*, 1996, **510**, 219; F. Neve, A. Crispini and O. Frascangelli, *Inorg. Chem.*, 2000, **39**, 1187.
- 11 R. Uson, J. Forries, M. A. Uson, J. F. Yaguee, P. G. Jones and K. Meyer-Baese, *J. Chem. Soc., Dalton Trans.*, 1986, 947.
- 12 J. L. Graff and M. G. Romanelli, *J. Chem. Soc., Chem. Commun.*, 1987, 337.
- 13 A. C. Skapski and M. L. Smart, *Chem. Commun.*, 1970, 658.
- 14 J. M. Corker and J. Evans, *J. Chem. Soc., Chem. Commun.*, 1991, 1104; J. M. Corker, PhD Thesis, University of Southampton, 1990.
- 15 J. F. Fauvarque, F. Pfluger and M. Troupel, *J. Organomet. Chem.*, 1981, **208**, 419; C. Amatore and F. Pfluger, *Organometallics*, 1990, **9**, 2276; C. Amatore, A. Jutand, F. Khalil and L. Mottier, *Organometallics*, 1993, **12**, 3168.
- 16 M. Hagelstein, A. San Miguel, T. Ressler, A. Fontaine and J. Goulon, *J. de Physique IV*, 1997, **1**, C2–303.
- 17 N. Binsted, PAXAS Program for the analysis of X-ray absorption spectra, University of Southampton, 1988.
- 18 EXCURV98, CCLRC Daresbury Laboratory Computer Program, Cheshire, 1998.
- 19 J. M. Corker, J. Evans, H. Leach and W. Levason, *J. Chem. Soc., Chem. Commun.*, 1989, 181.
- 20 P. T. Beurskens, G. Admiraal, G. Beurskens, W. P. Bosman, S. Garcia-Granda, R. O. Gould, J. M. M. Smits, C. Smyskalla, PATTY, The DIRDIF Program System, Technical Report of the Crystallography Laboratory, University of Nijmegen, The Netherlands, 1992.
- 21 TeXsan: Crystal Structure Analysis Package, Molecular Structure Corporation, Houston, TX, 1992.